Mechanical Properties of TIG Welded AL-Zn-Mg Alloy

D. K. Singh[+], P. K. Ghosh[+], M. Breazu & L. Issler[×]

Welding of Al-Zn-Mg alloy has been carried out by using AG conventional continuous current and pulsed current and pulsed current Tungsten inert gas (TIG) welding processes. The influence of various welding parameters on the soundness of the weld was studied by estimation of flaws in it. The effect of flaw size present like a crack inside the weld on the tensile strength of the weld has been determined. The influence of flaw size on the fracture toughness of the weld deposit has also been studied. It has been observed that for small flaws the failure is net stress controlled, whereas for large flaws the failure has been found to be stress intensity controlled.

INTRODUCTION

The Al-Zn-Mg alloy for its large strength to weight ratio is being largely used for fabrication of light weight structures in the Aerospace and automobile industries, portable bridges etc. These applications in a number of cases employ welding as a primary tool for joining of components. In general the aluminium alloys are welded by using inert gas (MIG) and tungsten inert gas (TIG) welding processes. The TIG welding in fabrication of light weight structure is popular due to its simplicity in use, less hazardous in nature and good penetrating capacity in comparison to that of MIG welding process (1,2). But inspite of its simplicity, the use of TIG is largely confined to some special applications such as the root pass etc. due to its nature of significant heat building in the component (3,4). The heat build up widens the weld bead, coarsens the microstructures of weld deposit and also enhance the chance for development of porosity and flaws in weld deposit (3,5), which are harmful for the mechanical properties of weldment of high strength material.

In past few years the use of controlled rate of heat input in TIG welding achieved by introducing pulse current has gained a significant popularity. In pulse TIG welding the operating tolerance arises largely from the fact that the weld pool is allowed to solidify between pulses, and heat is dissipated in the work. As such the effect of heat buildup or disparity in heat sink is largely avoided (3). So the pulse frequency plays a significant role on quality of the weld (3, 4, 6, 7). so far a considerable amount of work has been carried out (3-8) to study the utility of pulse TIG welding in joining of components of various cross-section. However, the field still have paucity of data regarding the influence of porosity content and flaw size on the mechanical properties of the weld. In this work an effort has been made to understand these aspects, so that the utilisation of TIG welding process can be made more effective in case of joining of high strength aluminium alloys in which the fracture properties are considered as an important criteria for its use.

+ Welding Research Laboratory, Deptt. of Mechanical & Industrial Engg. University of Roorkee, Roorkee-247 667 +

× Fachhochschule für Technik Kanalstrasse 33, D-7300 Esslingen (FRG) ×

EXPERIMENTATION

TIG welding of extruded Al-Zn-Mg alloy (cross section 50×6.8 mm) was carried out under AC continuous current and pulsed current by using Al-Mg (1.2 mm dia) filler wire. Chemical composition of the base metal and filler wire are shown in Table I and II respectively.

Table I

Chemical composition of Base Metal

Element	Zn	Mg	Mn	Fe	Si	Cu	Al
Wt. %	4.5	1.25	0.45	0.4	0.3	0.15	rest

Table II

Chemical composition of Filler Wire

Element	Mg	Mn	Cr	Ti	Al
Wt. %	4.9	0.7	0.15	0.15	rest

The commercial argon of 99.97% purity was used as shielding gas. During welding the flow of argon was maintained between 15 to 18 *l*/min, using a gas nozzle of 18 mm dia. The torch, designed, for the mechanised

around the welding arc by a fine-mesh inserted inside the nozzle. The tungsten-thoriated electrode of dia. 4 mm was used. The entire experiments were carried out on the longitudinal pneumohydraulic clamping device, using a stainless steel back bar, and a mechanized torch movement. The joint preparation, the scheme of welding procedure and the seam section are shown in Fig.1. At the time of welding the wire feed speed was suitably adjusted to obtain an uniform bead

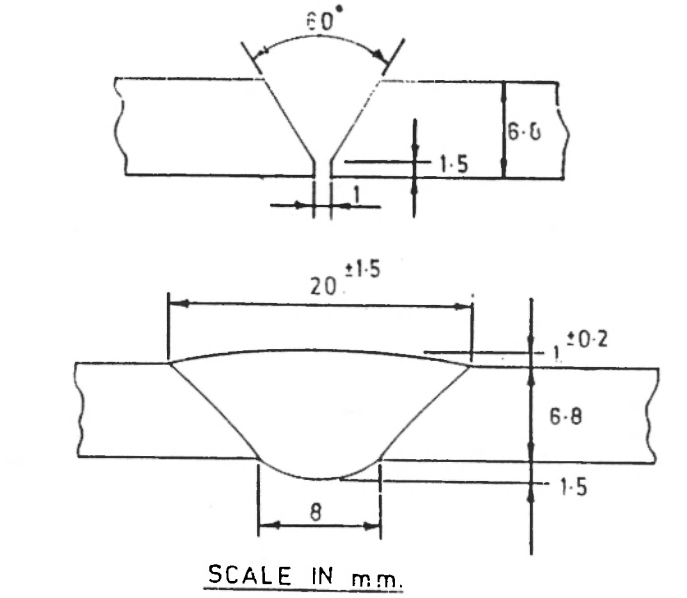

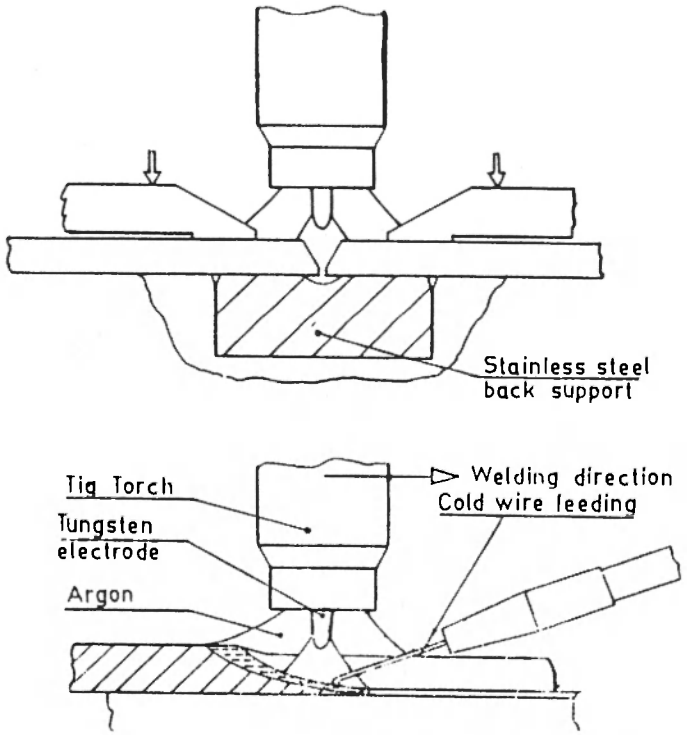

Fig. 1. Joint preparation and scheme of welding procedure

reinforcement of the order of 0.8-1.00 mm. During continuous current welding the welding current was varied from 200 to 266 Amp and in case of pulsed current welding the base and peak currents were varied within 200-239 Amp and 239-266 Amp respectively. The welding speed and pulse frequency were varied from 2.0-8.0 cm/min and 0-7.5 Hz respectively. From the weld length of 300 mm sufficient part was discarded from both the ends to avoid the defects resulting from the run on and run off of the arc.

For metallographic study the specimens were collected from the middle portion of the weldment and the transverse section of the specimens was prepared by standard metallographic procedure. The specimens were etched by Keller's reagent and studied under optical microscope.

The porosity content of weld deposit, appeared as black spots on the metallographically polished matrix, was determined by point counting method (9).

During welding at certain parameters some welds were found to develop cracks towards its root. Tensile specimens as schematically shown in Fig. 2 were

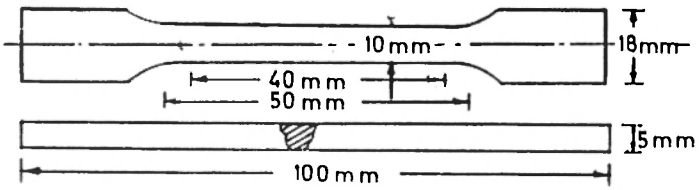

Fig. 2. Schematic diagram of tensile test specimen.

prepared, from the sound welds and also from the welds having crack, by keeping the weld region at its centre. The specimens were also collected from uncracked welds containing different level of porosity. The tensile test was carried out in a servohydraulically controlled universal testing machine at a cross head speed of 1 mm/min. during tensile test the load vrs. extension behaviour of the specimen was plotted in x-y recorder.

The area fraction of flaw in the specimen was estimated by standard metallographic process carried out on the fractured (predominantly of brittle nature) tensile

specimen. However, the flaw or crack size was measured under optical microscope viewing the transverse section of the weld joint as schematically shown in Fig. 3.

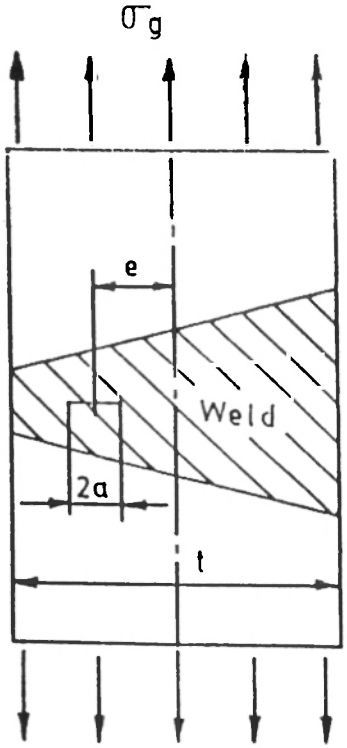

Fig. 3. Schematic diagram of eccentric crack panel.

The fracture toughness of weld deposit representing the resistance to unstable crack propagation in fracture process, was determined by using the specimens, containing a given level of porosity, having eccentrically located flaw towards the root of the weld. Thus, the stress intensity factor, K_1, was determined by flowing the procedure given in ASME XI, where for tensile load (Fig. 3).

$$K_1 = \sigma_g . M_m \sqrt{\pi . a/Q} \ N.mm^{3/2} \quad .....(i)$$

where

σ_g = Gross tensile strength

M_m = Membrane correction factor (ASME XI)

a = Half flaw size

Q = Shape factor of flaw (Q ≈ 1 in this case)

σ_g = P/A (N/mm^2) .....(ii)

where,

P = Ultimate tensile load

A = Total cross sectional area (t.w.)

t = Thickness of the specimen

w = Width of the specimen

The stress intensity factor at the moment of fracture assumed as pseudo-fracture toughness, K_1* is plotted as a function of flaw size (2a). For determining the M_m the eccentricity, E_c, of the location of flaw is estimated as

$$E_c = 2e/t \quad ...(iii)$$

where,

e = distance between the centre of the flaw and the centre of the specimen

Table III

Scheme of Welding Parameters

Base Current (Amp)	Peak Current (Amp)	Welding Speed (cm/min.)	Cold Wire (cm/min.)	Pulse Frequency Hz
200	—	2	110	0
239	—	6	330	0
266	—	8	440	0
200	239	4	220	0.5
200	239	4	220	2.5
200	239	4	220	4.0
200	239	4	220	5.5
220	239	4	220	7.5
220	266	6	330	0.5
220	266	6	330	2.5
200	266	6	330	4.0
220	266	6	330	5.5
220	266	6	330	7.5
239	266	8	440	0.5
239	266	8	440	2.5
239	266	8	440	4.0
239	266	8	440	5.5
239	266	8	440	7.5

RESULTS AND DISCUSSIONS

Typical macrophotograph of a sound joint having no flaw in weld deposit is presented in Fig. 4. The presence of eccentrically located flaw of different size in the weld

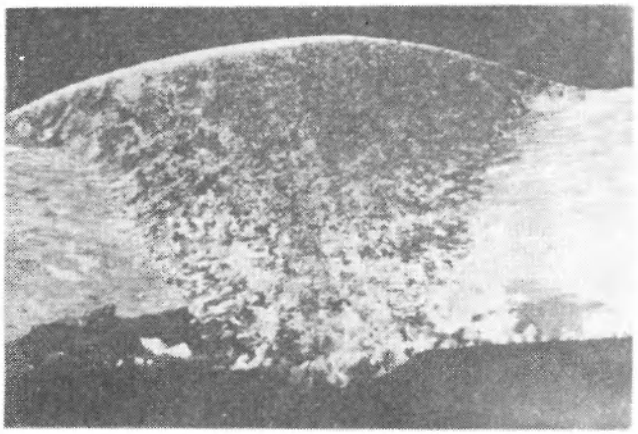

Fig. 4. Typical macrophotograph of sound weld, x5.

deposit as revealed in the fractograph of tensile specimens are shown in Fig. 5(i and ii). During

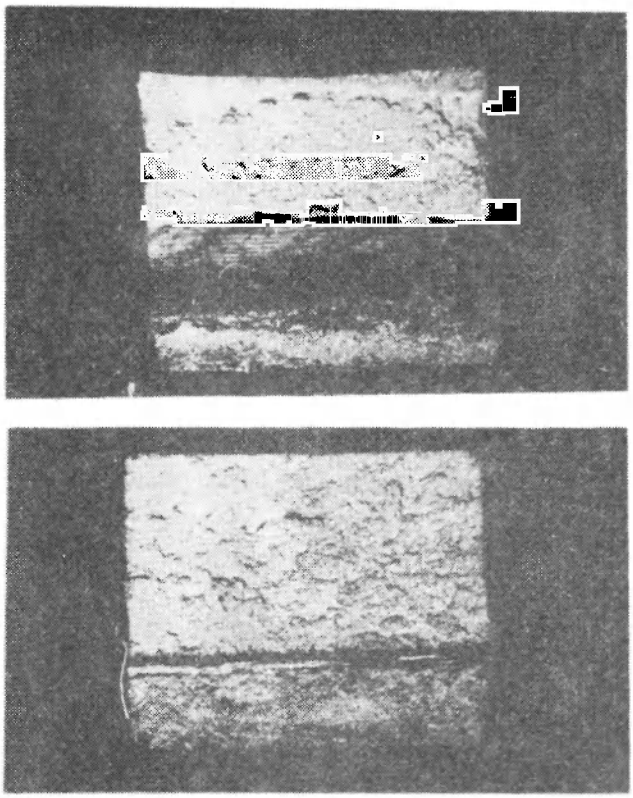

Fig. 5.(i & ii) Presence of eccentrically located crack in weld revealed in fractographs, x5.

continuous current TIG welding, the effect of variation in welding parameters on the area fraction of flaw (2a/w) in weld deposit is presented in Fig. 6. The histogram shows that the increase in welding current from 200 to

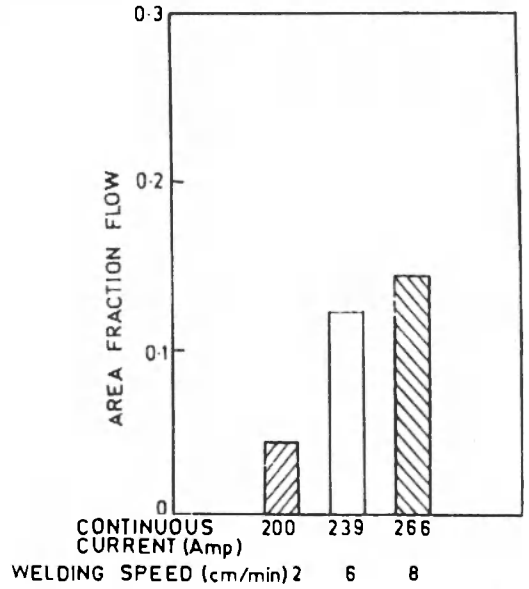

Fig. 6. The effect of continuous current welding; parameters on area fraction flaw.

266 Amps along with an increase in welding speed from 2 to 8 cm/min. increase the area fraction of flaw in weld deposit. During welding with pulsed current the effect of various pulse parameters on the area fraction of flaw is shown in Fig. 7. The figure shows that the area

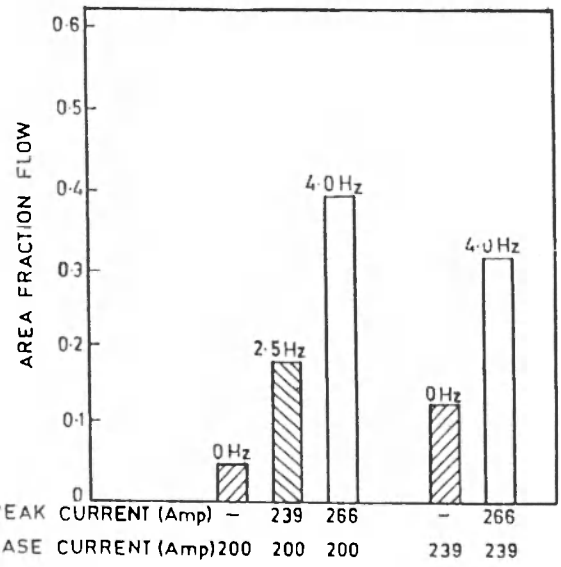

Fig. 7. The effect of pulse parameters on area fraction of flaw.

fraction of flaw in weld deposit enhances significantly when the pulse frequency of 4 Hz is sued. The flaws have generated in the weld joint possibly due to less heat

input and insufficient protection of shielding gas from the bottom of the weldment.

The typical microstructure of weld deposit has been shown in Fig. 8. The micrograph shows that the weld deposit is having certain amount of porosity in it.

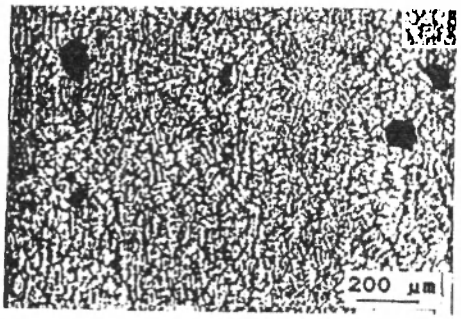

Fig. 8. Typical microstructure of weld deposit.

The influence of porosity content of weld deposit on the tensile strength of the same having no flaw (crack) has been shown in Fig. 9. The figure shows that the increase in porosity content beyond about 3.5 vol % reduces the tensile strength of weld deposit very slowly. This is in agreement to the earlier observation (10) which shows that in cast aluminium alloy the adverse effect of porosity content on tensile strength become relatively insignificant when the porosity level rises above a critical level of the order of 3-4 vol. %.

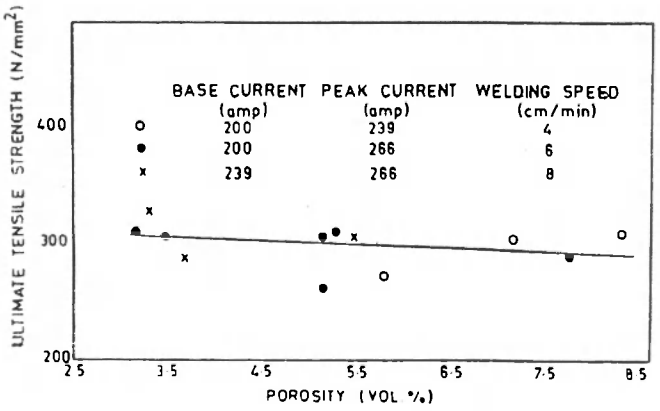

Fig. 9 Influence of porosity on tensile strength of weld deposit

The effect of flaw size on the gross ultimate tensile strength (σ_g) of the weld has been shown in Fig. 10. The load vrs. extension behaviour of specimens with and without flaw observed under tensile test is depicted in Fig. 11. The Fig. 10 shows that the presence of eccentrically located flaw in weld deposit having a size of the order of about 1.5 mm does not have a significant adverse effect on σ_g. However, a further increase in flaw size decreases the σ_g drastically.

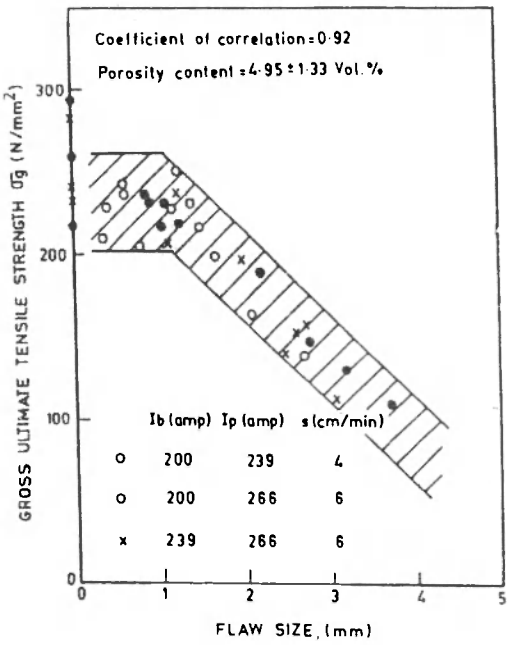

Fig. 10. The effect of flaw size on cross UTS of welds

To understand the behaviour of σ_g with the flaw size the fracture toughness characteristic of the welds has been studied. The influence of flaw size on the pseudo fracture toughness, K_1* of the weld deposit has been

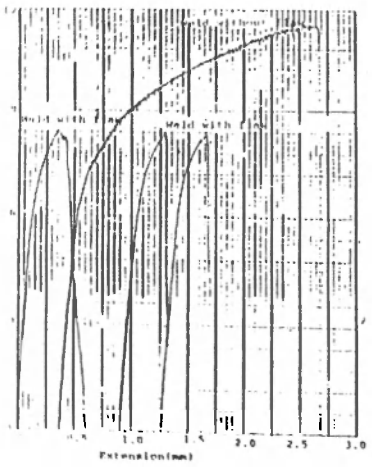

Fig. 11 Typical vrs. extension diagrams of the weld with and without flaw.

shown in Fig. 12. The figure shows that the curve approaches a constant value of about 350 $N/mm^{3/2}$ when the flaw size lies in the range of about 1.5 mm. This is in agreement to the earlier observation shown in Fig. 10. Thus it infers that for flaw size lower than about 1.5 mm the fracture is obviously not stress intensity controlled as depicted in Fig. 12. The fracture condition for small flaw (,1.5 mm) is governed by the nominal stress of about 200-250 N/mm^2 (Fig. 10) which can be denoted as collapse failure in ductile mode.

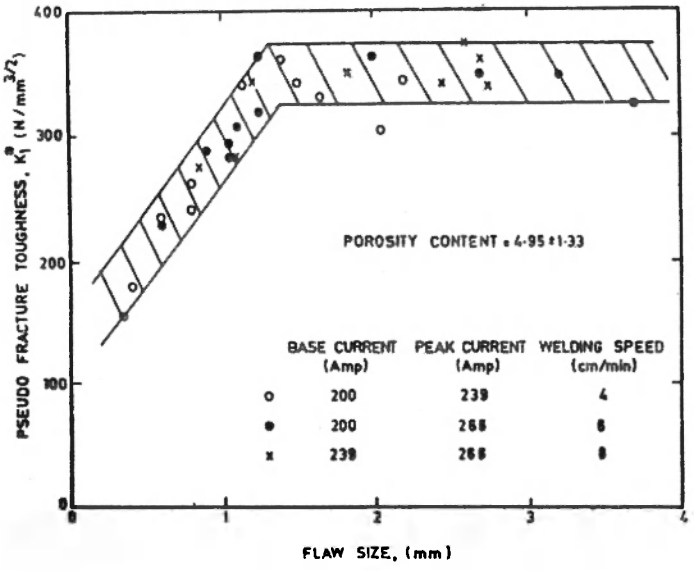

Fig. 12 Effect of flaw size on pseudo fracture toughness of weld deposit

CONCLUSION

The porosity content of weld deposit reduces the tensile strength of weld deposit considerably. However, in case of its level beyond about 3.5 vol. % it does not affect further the tensile strength of weld deposit significantly. In presence of crack like flaw, of size less than 1.5 mm, the weld deposit fractures in ductile mode, but when the flaw size increases further the failure takes place in brittle manner.

ACKNOWLEDGEMENT

The authors thankfully acknowledge the financial support given by the Council of Scientific and Industrial Research, New Delhi to carry out the present investigation.

REFERENCES

1. Welding Handbook, 7th ed. Vol. 2. AWS
2. Welding Handbook, 7th ed. Vol. 4, AWS.
3. J. C. Needham, "Pulsed current tungsten arc welding — an introduction to the process", Seminar handbook, The Welding Institute, Cambridge (1972).
4. A. W. Carter, "Pulsed TIG welding of pipes", Seminar Handbook, The Welding Institute, Cambridge (1972).
5. J. W. Wealaons and B. Allen, Met. Fab., 37, 5, (1969), 210.
6. A. G. Brain and S. C. Needham, BWRA Committee Report, A1/37/63.
7. A. W. Carter and J. A. Street, "Arc characteristics of pulsed A. C. TIG welding", Seminar Handbook, The Welding Institute, Cambridge (1972).
8. D. K. Singh, P. K. Ghosh and M. Breazu, Procd. Int. Conf. on Welding Tech., Sept. (1988), Univ. of Roorkee, India, III-109.
9. R. T. Dehoff and F. N. Rhines, Quantitative microscopy, McGraw Hill Book Co., New York, (1968), 70.
10. Radha Krishnan, Sheshan and Sheshadri, Trans. Ind. Inst. of Met., 34, 2, (1981), 169.